J|A|C|S
ARTICLES
Published on Web 11/22/2003

Direct Evaluation of a Mechanism for Activation of the RecA Nucleoprotein Filament

Alberto I. Roca and Scott F. Singleton*,†

Contribution from the Department of Chemistry and Department of Biochemistry and Cell Biology, Rice University, P.O. Box 1892 MS 65, Houston, Texas 77251-1892

Received May 23, 2002; E-mail: sfs@unc.edu

Abstract: The RecA protein of *Escherichia coli* controls the SOS response for DNA damage tolerance and plays a crucial role in recombinational DNA repair. The formation of a RecA·ATP·ssDNA complex initiates all RecA activities, and yet this process is not understood at the molecular level. An analysis of RecA·DNA interactions was performed using both a mutant RecA protein containing a tryptophan (Trp) reporter and oligodeoxyribonucleotides (ODNs) containing a fluorescent guanine analogue, 6-methylisoxanthopterin (6MI). Experiments using fluorescent ODNs allowed structurally distinct nucleoprotein filaments, formed in the absence and presence of ATPγS (a slowly hydrolyzed analogue of ATP), to be differentiated directly. Stopped-flow spectrofluorometry, combined with presteady-state kinetic analyses, revealed unexpected differences in the rates of RecA·ODN and RecA·ATPγS·ODN complex assembly. This is the first demonstration that such intrinsically fluorescent synthetic DNAs can be used to characterize definitively the real-time assembly and activation of RecA·ssDNA complexes. Surprisingly, the ssDNA binding event is almost 50-fold slower in the presence of the activating ATPγS cofactor. Furthermore, a combination of time-dependent emission changes from 6MI and Trp allowed the first direct chemical test of whether an inactive filament can isomerize to the active state. The results revealed that, unlike the hexameric motor proteins, the inactive RecA filament cannot *directly* convert to the active state upon ATPγS binding. These results have implications for understanding how a coincidence of functions—an ATP-communicated signal-like activity and an ATP-driven motorlike activity—are resolved within a single protein molecule.

Introduction

In living organisms, there is a dynamic balance between the need to preserve genomic information and the need to generate genetic diversity. The repair of damaged DNA is essential to the maintenance of heritable genetic information, while the variation of that information drives evolutionary adaptation. The *Escherichia coli* RecA protein mediates events in both pathways, and because its functions are conserved from bacteriophage to humans, its study has provided a paradigm for understanding these essential biological processes.[1] In addition to its roles in homologous recombination,[2] a process that allows horizontal gene transfer between species,[3] the RecA protein carries out at least two essential repair functions (Figure 1). First, RecA controls the SOS response for DNA damage tolerance via the formation of a complex between RecA and single-stranded DNA (ssDNA).[4] This "nucleoprotein filament" serves as an initiating signal for the derepression of many DNA repair genes[5] and the activation of translesion DNA synthesis.[6] In addition, RecA plays an indispensable role in restarting stalled replication forks,[7] possibly through recombinational DNA repair.[8] In this process, one of the two DNA molecules must have a single-stranded gap region to initiate assembly of the nucleoprotein filament.[9,10] This underscores the importance of ssDNA binding by RecA.

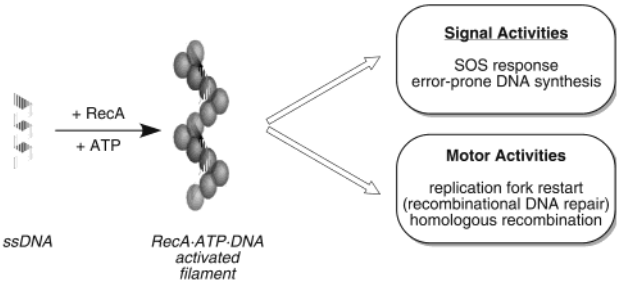

Figure 1. Cartoons depicting single-stranded DNA (ssDNA), the activated RecA·ssDNA nucleoprotein filament formed in the presence of ATP, and the two classes of activities mediated by the activated filament.

† Current address: Division of Medicinal Chemistry and Natural Products, School of Pharmacy, University of North Carolina at Chapel Hill, 305 A Beard Hall, CB #7360, Chapel Hill, NC 27599-7360.

(1) Cox, M. M.; Goodman, M. F.; Kreuzer, K. N.; Sherratt, D. J.; Sandler, S. J.; Marians, K. J. *Nature* **2000**, *404*, 37−41.
(2) Bianco, P. R.; Tracy, R. B.; Kowalczykowski, S. C. *Front. Bioscience* **1998**, *3*, D570−D603.
(3) Radman, M.; Taddei, F.; Matic, I. *Cold Spring Harb. Symp. Quant. Biol.* **2000**, *65*, 11−19.
(4) Friedberg, E. C.; Walker, G. C.; Siede, W. *DNA Repair and Mutagenesis*; ASM Press: Washington, DC, 1995; pp 407−464.
(5) Sassanfar, M.; Roberts, J. W. *J. Mol. Biol.* **1990**, *212*, 79−96.
(6) Goodman, M. F. *Trends Biochem. Sci.* **2000**, *25*, 189−195.
(7) Courcelle, J.; Ganesan, A. K.; Hanawalt, P. C. *BioEssays* **2001**, *23*, 463−470.
(8) Roca, A. I.; Cox, M. M. *Prog. Nucl. Acid Res. Mol. Biol.* **1997**, *56*, 129−223.
(9) Das Gupta, C.; Shibata, T.; Cunningham, R. P.; Radding, C. M. *Cell* **1980**, *22*, 437−446.
(10) West, S. C.; Cassuto, E.; Mursalim, J.; Howard-Flanders, P. *Proc. Natl. Acad. Sci. U.S.A.* **1980**, *77*, 2569−2573.

10.1021/ja0270165 CCC: $25.00

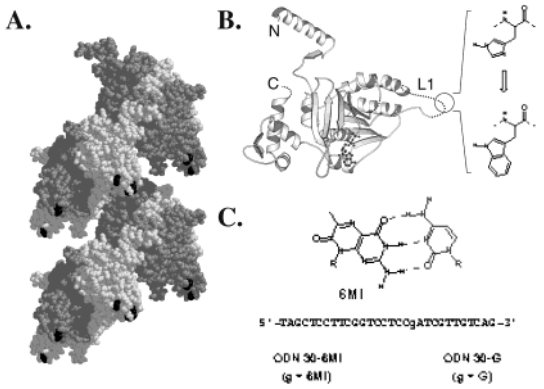

Figure 2. (A) Structure of the RecA protein filament where consecutive monomers are shown in alternating shades of gray and the two native Trp residues are shown in black. (B) RecA protein monomer displayed as a ribbon model. The approximate position of His163 in loop L1 as well as the N- and C-termini are indicated. (C) Structures of the ODNs investigated; the 6-methylisoxanthopterin base (6MI) is shown as a Watson−Crick pair with C (gray). The coordinates used to produce this figure were taken from the crystal structure of the RecA protein filament (Protein Data Bank accession code 1REA).

A combination of in vivo and in vitro studies suggests that, upon its activation by binding ATP, the complex formed between RecA protein and ssDNA plays a fundamental role in directing RecA function.

Multiple RecA monomers bind ssDNA sequence-independently, forming a multimeric right-handed filament with about six monomers per helical turn (Figure 2a). Electron microscopy (EM) defined two conformations of the RecA nucleoprotein filament whose DNA constituents have different helical geometries.[11] A "collapsed" filament (pitch ≈ 75 Å) forms in the absence of a cofactor or with ADP. An "extended" filament (pitch ≈ 95 Å) forms with nonhydrolyzable analogues of ATP such as adenosine 5′-*O*-(3-thiotriphosphate) (ATPγS). The extended nucleoprotein filament has two DNA binding sites with binding site sizes of three nucleotides (nts) per RecA monomer. The extended conformer with DNA bound at the primary site ("site I") is the active form of the RecA nucleoprotein filament since the quaternary complex formed between RecA protein, ssDNA, ATPγS, and Mg^{2+} in vitro comprises the inducing signal for SOS[12] and forms the recombination machinery that pairs and exchanges homologous DNA strands.[13,14] To address fundamental issues concerning the initiation of DNA repair processes, the mechanisms of formation and activation of the key RecA·ssDNA intermediate must be established.

Ideally a kinetic description of nucleoprotein filament assembly and activation will account for the remarkably diverse functionality displayed by this relatively small protein (M_r 37 842; 352 amino acids). In particular, RecA directs an ATP-dependent DNA strand exchange reaction in vitro that serves as a model system for the in vivo process of recombinational repair. In this context, RecA is thought to function as a molecular motor that transduces ATP binding energy via ligand-induced filament structural changes to the DNA rotation that allows strand pairing and exchange.[15] The RecA core domain can be

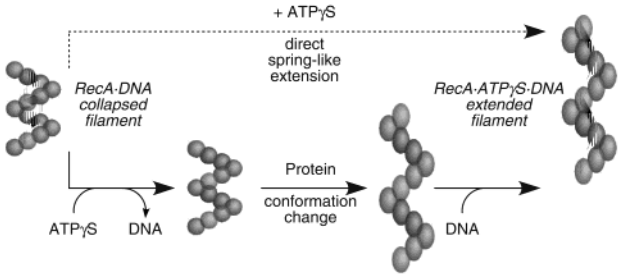

Figure 3. Cartoons depicting alternative mechanisms for activation of collapsed RecA·DNA filament by ATPγS. The upper path represents the "accordion model", while the lower path summarizes a plausible stepwise mechanism involving RecA·DNA dissociation followed by reassociation.

considered a fundamental component of other molecular motors such as the F_1-ATPase[16] and hexameric DNA helicases,[17,18] and all members of these protein families share pseudo-six-fold symmetric structures.[19,20] Although RecA can form planar hexameric rings such as those of the motor proteins,[21−24] such RecA rings do not bind DNA, and no function has been uniquely ascribed to this quaternary state.[25,26] All available evidence indicates that RecA protein is active only as the extended helical filament (described above; Figure 2) in complex with ssDNA and ATP(γS). Structural models derived from EM argue strongly against the possibility that the RecA hexameric rings are intermediates in RecA filament assembly and emphasize that the rings are structural rather than functional analogues of the hexameric motor proteins.[25,26]

The fact that the active RecA protomer serves in a signaling capacity and is structurally characterized as a helical filament rather than a planar ring led us to question whether RecA's putative motor function would be analogous to those of the F_1-ATPase and hexameric helicases. A common mechanistic feature of the latter proteins is the observation that the "inactive" nucleotide-free state is readily converted to the "active" state by rapid saturation of the nucleotide-binding sites followed by a presteady-state burst of NTP hydrolysis at a limited number of active sites to yield the steady-state Michaelis complex. During the activation process, protein monomers undergo conformational changes that are thought to reflect those necessary during each molecular motor's work cycle. If the helical RecA filament were to undergo such an activation, it would require a springlike extension of the helix (Figure 3, upper pathway). Such a conformational change of the multimeric filament has been described by an "accordion" model.[27,28]

(11) Egelman, E. H.; Stasiak, A. *Micron* **1993**, *24*, 309−324.
(12) Little, J. W.; Edmiston, S. H.; Pacelli, L. Z.; Mount, D. W. *Proc. Natl. Acad. Sci. U.S.A.* **1980**, *77*, 3225−3229.
(13) Honigberg, S. M.; Gonda, D. K.; Flory, J.; Radding, C. M. *J. Biol. Chem.* **1985**, *260*, 11845−11851.
(14) Menetski, J. P.; Bear, D. G.; Kowalczykowski, S. C. *Proc. Natl. Acad. Sci. U.S.A.* **1990**, *87*, 21−25.
(15) MacFarland, K. J.; Shan, Q.; Inman, R. B.; Cox, M. M. *J. Biol. Chem.* **1997**, *272*, 17675−17685.
(16) Abrahams, J. P.; Leslie, A. G. W.; Lutter, R.; Walker, J. E. *Nature* **1994**, *370*, 621−628.
(17) Sawaya, M. R.; Guo, S.; Tabor, S.; Richardson, C. C.; Ellenberger, T. *Cell* **1999**, *99*, 167−177.
(18) Singleton, M. R.; Sawaya, M. R.; Ellenberger, T.; Wigley, D. B. *Cell* **2000**, *101*, 589−600.
(19) Egelman, E. *Trends Biochem. Sci.* **2000**, *25*, 183−184.
(20) Egelman, E. *Trends Biochem. Sci.* **2000**, *25*, 179−182.
(21) Brenner, S. L.; Zlotnick, A.; Griffith, J. D. *J. Mol. Biol.* **1988**, *204*, 959−972.
(22) Heuser, J.; Griffith, J. *J. Mol. Biol.* **1989**, *210*, 473−484.
(23) Brenner, S. L.; Zlotnick, A.; Stafford, W. F. *J. Mol. Biol.* **1990**, *216*, 949−964.
(24) Benight, A. S.; Wilson, D. H.; Budzynski, D. M.; Goldstein, R. F. *Biochimie* **1991**, *73*, 143−155.
(25) Yu, X.; Angov, E.; Camerini-Otero, R. D.; Egelman, E. H. *Biophys. J.* **1995**, *69*, 2728−2738.
(26) Yu, X.; Egelman, E. H. *Nat. Struct. Biol.* **1997**, *4*, 101−104.
(27) Dunn, K.; Chrysogelos, S.; Griffith, J. *Cell* **1982**, *28*, 757−765.
(28) Roca, A. I.; Cox, M. M. *CRC Crit. Rev. Biochem. Mol. Biol.* **1990**, *25*, 415−456.

A rigorous investigation of the molecular events involved in the formation of the RecA·ssDNA complex is necessary to obtain a comprehensive understanding of the possible ways by which this recombination molecular motor initiates and regulates DNA repair processes. Toward this end, we report the extension of our recent work using intrinsically fluorescent synthetic DNA[29,30] for the mechanistic elucidation of RecA nucleoprotein filament assembly and activation. The fluorescence properties of 6-methylisoxanthopterin 2′-deoxynucleoside (d6MI, Figure 2c) are sensitive to its microenvironment, such that oligodeoxyribonucleotides (ODNs) containing d6MI in place of a single dG residue (30-6MI, Figure 2c) allow the structurally distinct nucleoprotein filaments formed in the absence and presence of ATPγS (a slowly hydrolyzed analogue of ATP) to be differentiated. Stopped-flow spectrofluorometry, combined with pre-steady-state kinetic analyses, revealed unexpected differences in the rates of RecA·ODN and RecA·ATPγS·ODN complex assembly. To our knowledge, this is the first demonstration that such intrinsically fluorescent synthetic ODNs can be used to characterize definitively the assembly and activation of RecA·ssDNA complexes. Finally, a combination of time-dependent emission changes—from fluorophores intrinsic to both DNA (d6MI) and protein (Trp)—allowed the first direct chemical test of whether the collapsed filament can isomerize to the active state. The results revealed that, unlike the hexameric motor proteins, the inactive RecA filament cannot *directly* convert to the active state upon ATPγS binding. These results have implications for understanding how a coincidence of functions—an ATP-communicated signal-like activity and an ATP-driven motorlike activity—are resolved within a single protein molecule.

Results and Discussion

At a minimum, any solution-phase method to analyze RecA nucleoprotein filaments must recapitulate the structural characteristics and their dependence on ATP, described in the Introduction (Figure 3). Although the use of DNA fluorescence and spectrofluorometry provides a potentially versatile, solution-phase method for monitoring RecA·ssDNA complexes, the natural DNA bases are only minimally luminescent.[31] Moreover, stoichiometric amounts of RecA protein coat the DNA molecule because RecA is not an enzyme with respect to its DNA binding activity. Such high protein levels produce substantial light scattering, and the accompanying high tryptophan levels lead to a large background fluorescence problem. Historically, two approaches have been used to overcome these issues: conjugation of the DNA to an extrinsic fluorophore and the use of *multiple* fluorescent base analogues. Extrinsic fluorophores such as fluorescein have been used to study RecA·DNA interactions.[32−37] However, an extrinsic fluorophore's signal reflects the microenvironment of the dye rather than that of the DNA,[38] and there is indication that fluorescein changes the DNA binding activity of the RecA protein.[30,32] The need for DNA-based signals can only be addressed using synthetic DNA analogues. To date, the use of fluorescent nucleosides in ODNs has involved *multiple* 1,N^6-ethenoadenine (ϵA),[39] 2-aminopurine (2AP),[40,41] or 5-methylpyrimidin-2-one (M5K)[29] monomers due to their ultraviolet excitation and low quantum yields in DNA ($\sim$0.02).[42,43]

Recently, we provided proof of principle for monitoring the dynamics of RecA·ssDNA interactions using intrinsic DNA fluorescence. RecA·DNA complexes were quantitatively analyzed using ODNs as short as 60 nts containing the intrinsically fluorescent pyrimidine base M5K in place of three specific cytosine residues.[29] Subsequently, we demonstrated that 30mer ODNs with *single* d6MI nucleotides were sufficient for the characterization of RecA·ssDNA complexes.[30] The photophysics of this fluorescent DNA reporter—6MI is a relatively bright fluorophore in ssDNA (quantum yield $\approx$ 0.3), and its emission peak is red-shifted from a protein's tryptophan signal—are ideally suited to monitor a DNA strand's microenvironment in RecA nucleoprotein filaments.[44] The ODNs containing single 6MI fluorophores demonstrated features characteristic of DNA bound by the RecA protein. Moreover, the use of short ODNs maximizes the proportion of fluorophore in the ODN and emphasizes local RecA monomer·DNA interactions while minimizing long-range effects such as cooperativity.

Steady-State Emission of ODNs Containing a Single 6MI Base. Figure 4 shows the steady-state fluorescence emission spectra of 0.1 μM (3 μM-nts) ODN 30-6MI in the absence and presence of saturating amounts of RecA.[45] For comparison, the spectrum of the ODN following complete hydrolysis to its constituent nuleotides (i.e., free d6MI) using Exonuclease I is also plotted. The emission of the d6MI fluorophore within an ODN is quenched $\sim$80% relative to the free nucleoside, presumably due to intramolecular base stacking within the DNA strand.[44] Upon RecA addition to ODN 30-6MI in the absence of ATPγS, a $\sim$2-fold enhancement of the ODN's emission was observed (Figure 4), providing a direct spectroscopic measurement of RecA·DNA complex formation. In the presence of RecA·ATPγS, the intensity of the ODN 30-6MI emission is also increased $\sim$2-fold. Furthermore, the maximum is blue-shifted approximately 8 nm. The conclusion that these spectroscopic changes are the result of RecA·DNA complex formation is supported by the observation that the emission changes are saturatable and replicated by fluorescence anisotropy measurements (see below).

(29) Singleton, S. F.; Shan, F.; Kanan, M. W.; McIntosh, C. M.; Stearman, C. J.; Helm, J. S.; Webb, K. J. *Org. Lett.* **2001**, *3*, 3919−3922.
(30) Roca, A. I.; Hawkins, M. E.; Singleton, S. F. Submitted for publication.
(31) Daniels, M.; Hauswirth, W. *Science* **1971**, *171*, 675−677.
(32) Volodin, A. A.; Smirnova, H. A.; Bocharova, T. N. *FEBS Lett.* **1994**, *349*, 65−68.
(33) Wittung, P.; Ellouze, C.; Maraboeuf, F.; Takahashi, M.; Nordén, B. *Eur. J. Biochem.* **1997**, *245*, 715−719.
(34) Sjöback, R.; Nygren, J.; Kubista, M. *Biopolymers* **1998**, *46*, 445−453.
(35) Ellouze, C.; Selmane, T.; Kim, H. K.; Tuite, E.; Nordén, B.; Mortensen, K.; Takahashi, M. *Eur. J. Biochem.* **1999**, *262*, 88−94.
(36) Bar-Ziv, R.; Libchaber, A. *Proc. Natl. Acad. Sci. U.S.A.* **2001**, *98*, 9068−9073.
(37) Gourves, A. S.; Defais, M.; Johnson, N. P. *J. Biol. Chem.* **2001**, *276*, 9613−9619.
(38) Norman, D. G.; Grainger, R. J.; Uhrin, D.; Lilley, D. M. *Biochemistry* **2000**, *39*, 6317−6324.
(39) Bujalowski, W.; Jezewska, M. J. *J. Mol. Biol.* **2000**, *295*, 831−852.
(40) Raney, K. D.; Sowers, L. C.; Millar, D. P.; Benkovic, S. J. *Proc. Natl. Acad. Sci. U.S.A.* **1994**, *91*, 6644−6648.
(41) Bjornson, K. P.; Moore, K. J. M.; Lohman, T. M. *Biochemistry* **1996**, *35*, 2268−2282.
(42) Bloom, L. B.; Otto, M. R.; Beechem, J. M.; Goodman, M. F. *Biochemistry* **1993**, *32*, 11247−11258.
(43) Hawkins, M. E. *Cell Biochem. Biophys.* **2001**, *34*, 257−281.
(44) Hawkins, M. E.; Pfleiderer, W.; Balis, F. M.; Porter, D.; Knutson, J. R. *Anal. Biochem.* **1997**, *244*, 86−95.
(45) The RecA protein is required at a stoichiometric, rather than catalytic, relative concentration. (The nominal binding site size of a RecA monomer being 3 nts, each 30-nt ODN will be bound by 10 RecA monomers.) The concentration of the ODN is expressed in terms of moles of nucleotides per unit volume (e.g., μM-nts) to facilitate comparison of the relevant concentrations. Therefore, a 3 μM-nts solution of ODN will require a minimum RecA concentration of 1 μM, regardless of ODN length.

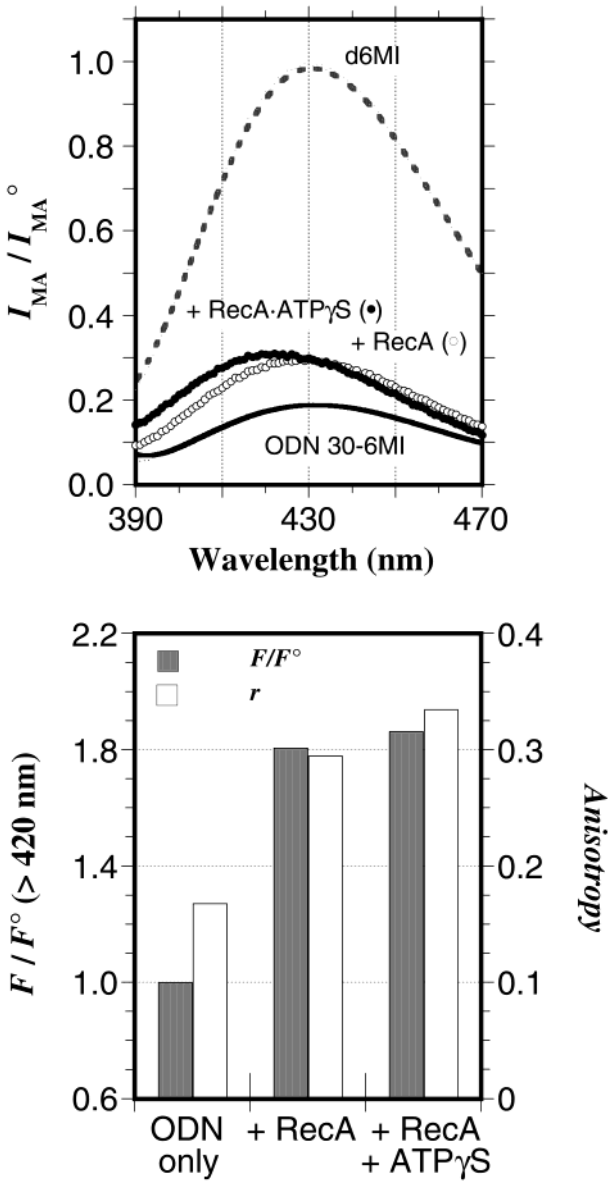

Figure 4. Influence of RecA and ATPγS on the total and polarized fluorescence emission of ODN 30-6MI. (A) Normalized fluorescence emission spectra, collected using excitation and emission polarizers oriented at 54.7° relative to one another ("MA" = magic angle), for the ODN alone (black line) or in the presence of either RecA (open symbols) or RecA and ATPγS (filled symbols). The spectrum of the ODN following complete hydrolysis to its constituent nuleotides (i.e., free d6MI) using Exonuclease I is also shown for comparison (dashed line). (B) Normalized total emission intensities ($F/F°$) and fluorescence anistropies [$r = (I_{||} - I_{\perp})/(I_{||} + 2I_{\perp})$] collected for the ODN alone (ODN) or in the presence of either RecA (+ RecA) or RecA and ATPγS (+ RecA + ATPγS).

The fluorescence emission of 30-6MI is sensitive to the formation of the collapsed versus the extended RecA·ssDNA complexes. The binding of RecA protein to 30-6MI causes an enhancement of the fluorescence intensity without affecting the emission peak maximum of the pteridine fluorophore. Such a signal change can be attributed to the reduction of quenching processes due to the fluorophore encountering a nonpolar binding site or the partial destacking of the fluorophore from neighboring aromatic bases. Although little is known about the ssDNA structural changes in the collapsed RecA filament, the RecA protein apparently induces only small changes in ssDNA conformation.[46]

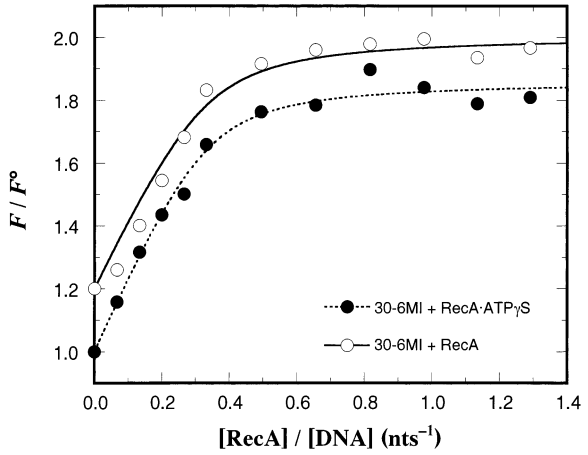

Figure 5. Total fluorescence titrations of ODN 30-6MI with RecA. DNA and RecA were incubated in either the absence (open symbols) or presence (filled symbols) of ATPγS prior to mixing. The former data set has been offset vertically by 0.2 units for clarity. The smooth curve represents the best fit to the equation described in the Experimental Section.

In contrast to the spectral properties of the collapsed filament, the ATPγS-induced extended RecA filament results in an 8-nm blue shift of the emission maximum in addition to a similar enhancement of the fluorescence intensity. The increase in fluorescence intensity is consistent with the well-documented DNA base destacking that occurs in the extended RecA·ssDNA filament.[11] However, the structural origins of the change in the fluorophore emission maximum remain unresolved.

The use of ATPγS instead of ATP raises the issue of the biological relevance of the results described herein. However, a variety of experiments have established that RecA·DNA complexes formed in the presence of ATPγS have structures[11] and activities[13,14] essentially identical to those complexes formed with ATP. Thus, the nucleoprotein filaments formed in the presence of ATPγS are well suited for the investigation of mechanistic questions.[30]

Quantitative Evaluation of RecA·ODN Complexes by Steady-State Spectrofluorometry. Monitoring DNA emission as a function of increasing protein concentration provided evidence that the signal change saturates and allowed characterization of the thermodynamics of RecA·DNA complex formation (Figure 5). In the presence of ATPγS and in the absence of cofactor, the RecA·DNA association was characterized by tight binding ($K_d \leq 40$ nM). An equivalence point analysis[47] of the DNA binding isotherms in Figure 5 yielded a DNA nts to RecA monomer ratio of 2.5 ± 0.3 in the absence of cofactor for ODN 30-6MI. In the presence of ATPγS, the value was 2.5 ± 0.4. Because the complexes between RecA and 30-6MI are characterized by the canonical 1:3 RecA monomer to nts stoichiometry determined by other techniques,[8] the ssDNA binding isotherms in Figure 5 provide evidence that d6MI does not disturb RecA·ssDNA interactions.

This observation provides a definitive advantage of the 6MI fluorophore over other DNA base analogues. In particular, polynucleotides containing ϵA, one of the most commonly used and readily accessible fluorescent base replacements, show a stoichiometry of 1:6 resulting from two ssDNA molecules binding RecA.[48,49] In addition, while the adenine analogue 2AP

(46) Takahashi, M.; Kubista, M.; Nordén, B. *J. Mol. Biol.* **1989**, *205*, 137−147.
(47) Silver, M. S.; Fersht, A. R. *Biochemistry* **1982**, *21*, 6066−6072.

has been used in an extensive variety of biochemical experiments, DNA molecules containing single-site[30] or multiple[29] 2AP substitutions are not suited to the quantitative characterization of RecA·ssDNA complexes.[50]

Distinguishing Active and Inactive Filaments using Fluorescence Anisotropy. The fluorescence of ODN 30-6MI serves as a sensitive indicator of RecA·ssDNA complex formation. However, the lack of a diagnostic difference in fluorescence intensity between the collapsed and extended RecA·DNA complexes led us to explore other fluorescence observables. The binding of RecA protein to the ODN results in an increase in the extent of polarization of the emission from 30-6MI (Figure 4). Specifically, the anisotropy of the free 30-6MI ODN was 0.168 ± 0.006, and this value increased to 0.295 and 0.335 for the RecA·30-6MI complexes formed in the absence and presence of ATPγS, respectively. Fluorescence anisotropy measurements as a function of RecA concentration (data not shown) parallel the previously observed emission intensity signal changes, substantiating the conclusion that the emission intensities provide an authentic signal for complex formation. Upon comparing the spectrofluorometric characteristics of the collapsed and extended RecA·ssDNA complexes, the combination of fluorescence anisotropy and emisison peak differences provide unambiguous evidence that the fluorescence of 6MI distinguishes the structurally unique filaments.

Presteady-State Analysis of RecA·ssDNA Collapsed Filament Formation Using Intrinsic DNA Fluorescence. The equilibrium analysis of RecA·ssDNA complexes described above recapitulated structural and thermodynamic differences that depended on the presence and identity of bound cofactor. We wondered whether these steady-state energetic differences would be reflected in the kinetics of nucleoprotein filament assembly or disassembly or both. Such differences would have important mechanistic implications for the assembly of the active nucleoprotein filament. Thus, we turned to a real-time analysis of complex assembly.

Rapid stopped-flow mixing of ODN 30-6MI (3 μM-nts)[51] with RecA (1.5−7.5 μM) results in a pre-steady-state emission increase (Figure 6). In contrast, there is no signal change when RecA binds nonfluorescent ODN 30-G, demonstrating the lack of any tryptophan fluorescence background. The time-dependence of the fluorescence intensity was best described by a single-exponential function. The relaxation time (τ) of this signal change was dependent on RecA concentration. Indeed, the observed reciprocal relaxation times demonstrated a linear dependence on the RecA concentration (Figure 7a). We conclude that this behavior is consistent with the simple, one-step, reversible association described by Scheme 1, where R° represents a RecA monomer, D represents a ssDNA nt, m is the number of protein monomers per filament, and n represents the number of nts bound by a single RecA monomer. Fitting the plot of pseudo-first-order rate constants ($k_{obs} = \tau^{-1}$) as a function of [RecA] allowed the determination of an intrinsic bimolecular association rate constant $k_1 = (1.1 \pm 0.2) \times 10^7$ $M^{-1}\cdot s^{-1}$ and a unimolecular dissociation rate constant $k_{-1} = 3.5 \pm 3.2\ s^{-1}$ (Figure 7a) at 37 °C.

The second-order rate constant for the assembly of the collapsed filament on ODN 30-6MI is similar to that observed

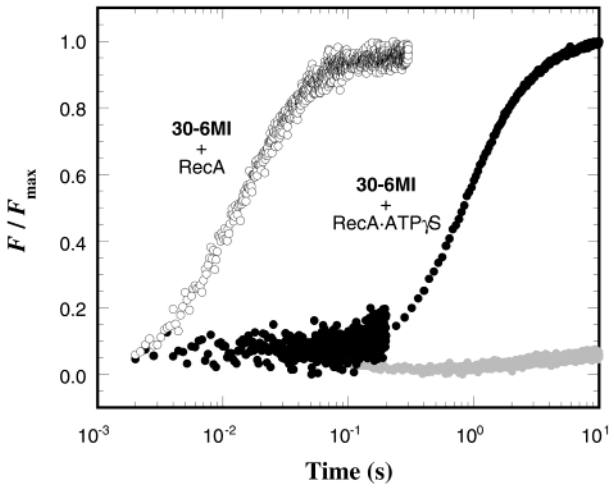

Figure 6. Real-time relative total emission (F/F_{max}) of ODN 30-6MI (black symbols) or 30-G (gray line) upon stopped-flow mixing with RecA. DNA and RecA were incubated in either the absence (open symbols) or presence (filled symbols) of ATPγS prior to mixing. The data shown for ODN 30-6MI are well described by single-exponential functions.

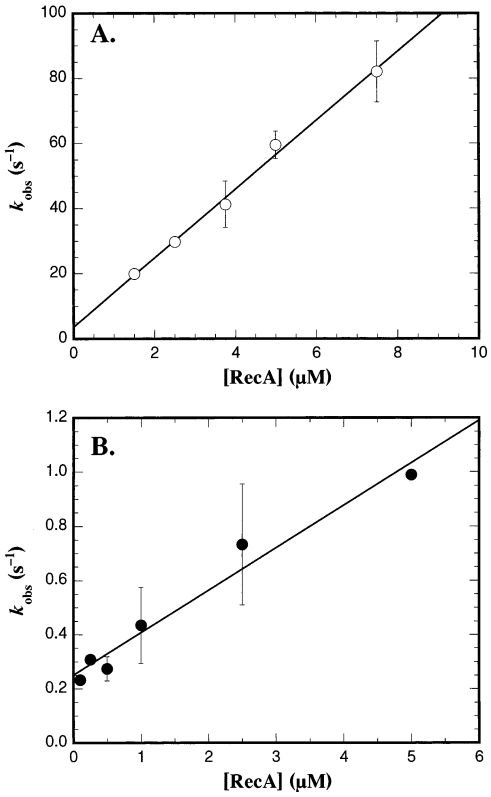

Figure 7. (A) Pseudo-first-order rate constants for RecA + ODN 30-6MI association plotted as a function of [RecA], and the best linear fits using the equation $k_{obs} = k_1[\text{RecA}] + k_{-1}$. (B) Pseudo-first-order rate constants for RecA·ATPγS + ODN 30-6MI association plotted as a function of [RecA], and the best linear fits using the equation $k_{obs} = k_2[\text{RecA}] + k_{-2}$.

Scheme 1

$$m\,\mathbf{R}^{\circ} + n\,\mathbf{D} \underset{k_{-1}}{\overset{k_1}{\rightleftharpoons}} (\mathbf{R}^{\circ}\cdot\mathbf{D}_n)_m$$

(48) Menetski, J. P.; Kowalczykowski, S. C. *J. Mol. Biol.* **1985**, *181*, 281−295.
(49) Zlotnick, A.; Mitchell, R. S.; Steed, R. K.; Brenner, S. L. *J. Biol. Chem.* **1993**, *268*, 22525−22530.
(50) A single 2AP substitution in dsDNA can cause local structural and dynamic perturbations. See: Nordlund, T. M.; Xu, D.; Andersson, S.; Nilsson, L.; Rigler, R.; Gräslund, A.; McLaughlin, L. W.; Gildea, B. *Proc. SPIE* **1990**, *1204*, 344−353.
(51) The concentrations of reactants after mixing are specified for stopped-flow experiments.

Scheme 2

$$m\,\mathbf{R}^{\mathrm{ATP}\gamma\mathrm{S}} + n\,\mathbf{D} \underset{k_{-2}}{\overset{k_2}{\rightleftharpoons}} (\mathbf{R}^{\mathrm{ATP}\gamma\mathrm{S}}\cdot\mathbf{D}_n)_m$$

previously for RecA binding to ϵA-labeled polynucleotides at 25 °C.[52] The value reported here is expressed in terms of RecA monomer concentration. The functional multimeric form of RecA that initiates binding to ssDNA is unknown. Under our solution conditions, RecA hexameric rings and stacks of rings are known to predominate.[21,24] Thus, to a first approximation, the second-order rate constant for the collapsed filament may represent a lower bound for an oligomeric protomer which binds ssDNA. Diffusional biomolecular association rates are typically between 10^6 and 10^8 $M^{-1}\cdot s^{-1}$.[53,54] Therefore, the bimolecular association of RecA and ODN 30-6MI is likely diffusion-controlled. The Rep and T7 helicases are also DNA-binding motor proteins whose association reactions are diffusion controlled.[41,55]

Presteady-State Analysis of RecA·ATPγS·ssDNA Extended Filament Formation Using Intrinsic DNA Fluorescence. Unexpectedly, ssDNA binding in the presence of ATPγS is much slower than that observed in its absence. When 3 μM-nts 30-6MI reacts with RecA (0.5−2.5 μM) in the presence of a saturating concentration of ATPγS (0.5 mM), the fluorescence of the ODN increases as expected. However, Figure 6 shows that 30-6MI binding by RecA in the presence of ATPγS occurs more than 50-fold more slowly than the association in the absence of cofactor. Nevertheless, the presteady-state fluorescence increase observed for mixing RecA·ATPγS with 30-6MI follows a simple exponential function, and the corresponding reciprocal relaxation times depend linearly on [RecA·ATPγS] (Figure 7b). Again, we infer a simple, one-step, reversible association reaction (Scheme 2, where $R^{ATP\gamma S}$ represents an ATPγS-bound RecA monomer, and D, *m*, and *n* are as described for Scheme 1). On the basis of the linear relationship between k_{obs} and RecA·ATPγS concentration, the second-order rate constant describing the formation of the extended RecA·ATPγS·ssDNA complex is $k_2 = (2 \pm 1) \times 10^5$ $M^{-1}\cdot s^{-1}$, and the first-order rate constant for its disassembly is $k_{-2} = 0.20 \pm 0.05$ s^{-1} (Figure 7b).

The bimolecular rate constant for RecA·ATPγS association with ssDNA reported here (2×10^5 $M^{-1}\cdot s^{-1}$) is much faster than that observed for RecA·ATPγS binding to ϵA-labeled DNA at 20 °C.[56] We note that RecA binds two molecules of ϵ-DNA and that the fluorescence signal changes monitored using this substrate were coincident with those from light scattering.[56] Hence, the molecular origins of the previously reported signal changes are not clear. Unfortunately, differences in experimental design (e.g., instrumental dead-time of <2 ms and >10 s for the current and previous reports, respectively) prevent a thorough comparison of the results.

A variety of experiments have established that the structures of the collapsed and extended RecA filaments are different,[11] and it has been generally accepted that the ATP cofactor activates the RecA protein. In particular the extended filament with a destacked DNA structure is thought to be a universally conserved helical scaffold necessary for the subsequent DNA pairing step of the recombination function of RecA.[57−61] However, the data in Figures 6 and 7 represent the first direct comparison of the kinetics of ssDNA binding by the RecA protein in the absence and presence of cofactor. To the best of our knowledge, the observation that ATPγS slows ssDNA binding was not predicted. This demonstrates the importance of kinetic studies for a complete understanding of the mechanism of RecA activation.

The presteady-state analysis reveals insights into the molecular events underlying RecA·ssDNA complex formation. There is precedence for a hexameric helicase with slow DNA binding steps in the DnaB protein of *E. coli*.[39] Although DnaB is structurally similar to RecA,[62] the rate of DnaB·ssDNA complex assembly is even slower (by ca. 10-fold) than the formation of the extended RecA filament. As the RecA protein can bind cofactor in the absence of DNA,[63,64] we assume that the RecA·ATPγS complex is preformed under the experimental conditions so that ATPγS binding is not rate-limiting. The fact that ATPγS slows RecA·ssDNA association has intriguing implications for the influence of ATPγS on the size of the RecA filament and the kinetics of possible rate-limiting RecA·ATPγS·ssDNA conformational changes.

One trivial reason for the reduced rate of ssDNA binding is that the ATPγS-bound RecA polymer has longer dimensions or comprises more monomers and therefore takes longer to diffuse than the cofactor-free RecA polymer. Likewise, ATPγS may induce a protomeric state of RecA that is not productive with respect to DNA binding. Such a state could result from the presence of either too few or too many monomers. Unfortunately, the effects of cofactor on the structure of the DNA-free RecA polymer yield contradictory predictions. In the absence of DNA, ATPγS induces a 30% increase in the helical pitch of the RecA filament.[65] In contrast, under conditions similar to those used here, binding of cofactor decreases the multimeric state of RecA filaments.[21,23,63] The absence of significant changes in light scattering over the course of our reactions (derived from mixing experiments, like that in Figure 6, with nonfluorescent ODN 30-G) suggests that there are little changes in the size or shape or both of the protein filament during the reactions. Thus, any changes in the multimeric state of RecA must not be substantial. When taken together with the data obtained from intrinsic protein fluorescence (see below), these facts lead us to the tentative conlusion that ATPγS-induced structural changes are unlikely to account for the 50-fold decrease in the rate of ssDNA binding observed in the presence of ATPγS.

(52) Silver, M. S.; Fersht, A. R. *Biochemistry* **1983**, *22*, 2860−2866.
(53) Northrup, S. H.; Erickson, H. P. *Proc. Natl. Acad. Sci. U.S.A.* **1992**, *89*, 3338−3342.
(54) Gabdoulline, R. R.; Wade, R. C. *Curr. Opin. Struct. Biol.* **2002**, *12*, 204−213.
(55) Picha, K. M.; Ahnert, P.; Patel, S. S. *Biochemistry* **2000**, *39*, 6401−6409.
(56) Chabbert, M.; Cazenave, C.; Hélène, C. *Biochemistry* **1987**, *26*, 2218−2225.
(57) Bertucat, G.; Lavery, R.; Prévost, C. *Biophys. J.* **1999**, *77*, 1562−1576.
(58) Egelman, E. H. *J. Mol. Biol.* **2001**, *309*, 539−542.
(59) Kosikov, K. M.; Gorin, A. A.; Zhurkin, V. B.; Olson, W. K. *J. Mol. Biol.* **1999**, *289*, 1301−1326.
(60) Shibata, T.; Nishinaka, T.; Mikawa, T.; Aihara, H.; Kurumizaka, H.; Yokoyama, S.; Ito, Y. *Proc. Natl. Acad. Sci. U.S.A.* **2001**, *98*, 8425−8432.
(61) Yu, X.; Jacobs, S. A.; West, S. C.; Ogawa, T.; Egelman, E. H. *Proc. Natl. Acad. Sci. U.S.A.* **2001**, *98*, 8419−8424.
(62) Yu, X.; Jezewska, M. J.; Bujalowski, W.; Egelman, E. H. *J. Mol. Biol.* **1996**, *259*, 7−14.
(63) Cotterill, S. M.; Fersht, A. R. *Biochemistry* **1983**, *22*, 3525−3531.
(64) Kowalczykowski, S. C. *Biochemistry* **1986**, *25*, 5872−5881.
(65) Ellouze, C.; Takahashi, M.; Wittung, P.; Mortensen, K.; Schnarr, M.; Nordén, B. *Eur. J. Biochem.* **1995**, *233*, 579−583.

An alternative explanation for the slow rate of RecA·ATPγS·ssDNA complex assembly is the existence of rate-limiting conformational changes which *precede* the formation of a stable complex. Our data suggest that such a conformational change likely occurs before the formation of the ternary RecA·ATPγS·ssDNA complex. Formally, a conformational change could involve a change in the DNA, the RecA protein, or the nucleoprotein filament. It is unlikely that such structural changes involve the ssDNA since base "breathing" and other fundamental motions occur on the order of microseconds and should therefore not be rate-limiting.[66] Thus, the RecA·ATPγS protein filament and a transient, initial RecA·ATPγS·ssDNA complex are the most likely candidates for the species involved in a rate-limiting conformational change.

The important inference from the results described above is that the *dynamics* of RecA·ssDNA interactions are fundamentally different during assembly of the inactive ("collapsed") and active ("extended") RecA filaments. Surprisingly, we observed that the inactive filament forms at a rate nearly 2 orders of magnitude faster than formation of the active filament. This observation directly leads to the question of whether the collapsed filament is an intermediate on the pathway to active filament formation. The resulting mechanistic model requires the formation of an intermediary RecA·ATPγS·ssDNA nucleoprotein filament in a collapsed state that would undergo subsequent conformational changes to form the extended filament. This mechanistic hypothesis is a simple restatement of the "accordion" model described in the Introduction (Figure 3) and establishes a putative mechanistic role for the inactive filament as a kinetic trap for ssDNA.

Such a function for the collapsed filament has been argued against on the basis of biochemical data for the RecA-catalyzed hydrolysis of ATP[67,68] and EM-derived structural data.[69] The latter report concluded that the DNA:RecA stoichiometry was distinctly different between the two classes of filaments. However, the EM data were collected using phage-derived DNA substrates different in length and structural complexity from the ODNs described herein. In contrast to the earlier results, our work with RecA·ODN complexes demonstrates that the two filaments formed in the presence and absence of ATPγS have the same stoichiometry of three nts per RecA monomer.[29,30] Taken together with our observation that the "inactive" collapsed filament binds ODNs at a substantially higher rate than the extended filament, these data led us to test *directly* the potential mechanistic role of the collapsed filament.

Presteady-State Analysis of RecA·ssDNA Filament Activation by Intrinsic DNA Fluorescence. The molecular origins of the influence of ATPγS on RecA·ssDNA interaction kinetics likely lay in the influence of ATPγS on the conformational dynamics of the protein-only or nucleoprotein filaments or both. If a transient, initial RecA·ATPγS·ssDNA nucleoprotein filament—in a collapsed-like state—has to undergo conformational changes to the final extended filament, we reasoned that the collapsed RecA·ssDNA filament would undergo a similar isomerization upon binding to ATPγS. Such a conformational change would be similar to the activation step of motor proteins. On the basis of the small changes in the steady-state emission spectra (Figure 4) and the rate constant for RecA·ATPγS·ssDNA association, we anticipated that such a conformational change would be revealed as a small intensity change occurring with a relaxation time near 2 s.

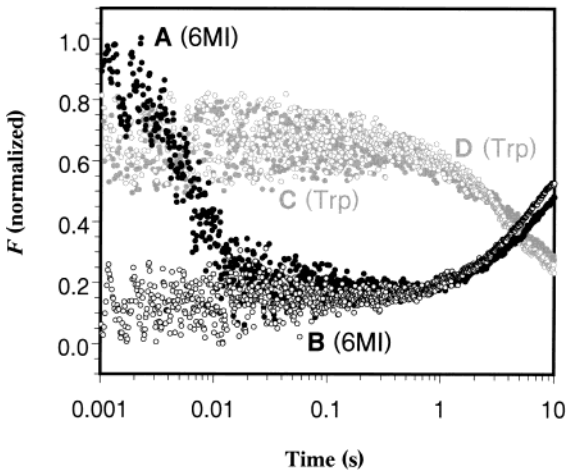

Figure 8. Real-time relative total emission (F/F_{max}) of ODN 30-6MI ("6MI", black symbols, traces A and B) or ^{H163W}RecA ("Trp", gray symbols, traces C and D) upon stopped-flow mixing of RecA·ssDNA filaments with ATPγS (filled symbols, traces A and C) or RecA·ATPγS with ssDNA (open symbols, traces B and D).

To address the issue of whether the RecA·ssDNA complex is an intermediate on the pathway to activated RecA·ATPγS·ssDNA formation, the RecA·30-6MI collapsed filament was rapidly mixed with ATPγS. Contrary to expectations, the intrinsic DNA emission demonstrated a dramatic decrease (relaxation time, $\tau \approx 6$ ms) followed by a 1000-fold slower increase back to the original signal level (Figure 8, trace A). Interestingly, the relaxation time and signal change for the slower phase coincided almost exactly with those observed when the binary RecA·ATPγS complex was mixed rapidly with ssDNA (Figure 8, trace B). We demonstrated above that the latter experiment directly monitors the bimolecular associaton between RecA·ATPγS and ssDNA. Moreover, comparison of the sign and magnitude of the emission changes during the more rapid phases with those revealed by the steady-state spectra suggests that the RecA·ssDNA complex dissociates upon mixing with ATPγS. Hence, the inactive RecA·ssDNA complex does not isomerize to the active RecA·ATPγS·ssDNA filament. These unambiguous observations lead to the remarkable inference that the collapsed filament is *not directly converted* to the active filament via springlike extension, but that it must disassemble and then reassemble in the active conformation.

The presteady-state data rule out the possibility that the more rapidly formed RecA·ssDNA complex serves as an intermediate for assembly of the more slowly formed active filament. Moreover, the relatively slow formation of the extended RecA·ATPγS·ssDNA filament cannot result from a rate-limiting conformational change of an intervening ternary complex in a collapsed conformation. This latter conclusion is consistent with the fact that a transient intermediate preceding RecA·ATPγS·ssDNA filament assembly was not observed (Figure 6). Because the d6MI fluorescence is highly sensitive to its microenvironment, it is unlikely that a preliminary collision complex formed without an accompanying d6MI emission change. We therefore conclude that a rate-limiting conformational change of the RecA·

(66) Porschke, D. *Eur. J. Biochem.* **1973**, *39*, 117−126.
(67) Lee, J. W.; Cox, M. M. *Biochemistry* **1990**, *29*, 7666−7676.
(68) Lee, J. W.; Cox, M. M. *Biochemistry* **1990**, *29*, 7677−7683.
(69) Yu, X.; Egelman, E. H. *J. Mol. Biol.* **1992**, *227*, 334−346.

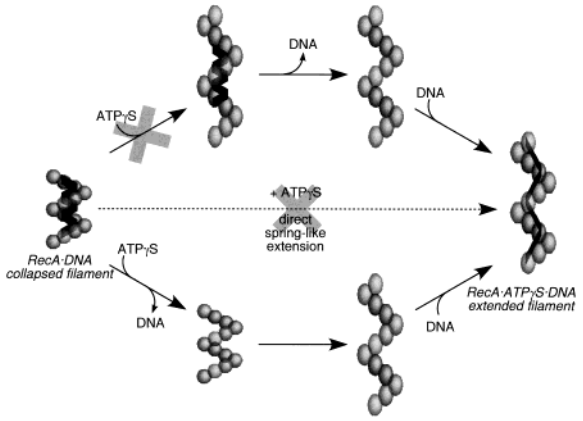

Figure 9. Cartoons depicting alternative mechanisms for activation of collapsed RecA·DNA filament by ATPγS. The two upper paths were ruled out by the results described herein. The most likely mechanism (lowest path) involves ATPγS-induced disassembly of the collapsed RecA·DNA filament followed by a conformational change of the protein-only filament that either immediately precedes or is concurrent with assembly of the extended nucleoprotein filament.

ATPγS protein filament is the most likely explanation for the unexpectedly slow binding of ssDNA by RecA·ATPγS.

Presteady-State Analysis of RecA·ssDNA Interactions by Intrinsic Protein Fluorescence. The transient-state spectral data described above demonstrate that the collapsed filament forms much more rapidly than the extended filament, but that the collapsed filament is not a competent intermediate on the pathway to formation of the active RecA·ATPγS·ssDNA filament. Any alternative mechanistic hypothesis for "activation" of the collapsed filament must now include the dissociation of the ssDNA from the inactive nucleoprotein filament as well as the filament conformational change (Figure 3, lower pathway). We envisaged two mutually exclusive kinetic schemes that describe the "activation" and have very different implications: protein conformational change could lead to ssDNA dissociation or ssDNA dissociation could lead to protein conformational change (Figure 9). To test these hypotheses, a signal for the RecA protein's conformation was required.

The native RecA tryptophans do not serve as reporters for ssDNA binding.[70−72] This limitation has been overcome by the substitution of Trp for nonfluorescent residues in the RecA protein.[73−76] Thus, we employed a previously described mutant RecA protein (^{H163W}RecA)[73,77] in which a Trp residue replaces a single His at residue position 163 in a putative DNA binding loop (Figure 2).[78] The fluorescence from this Trp residue reports on the conformational state of the protein (Figure 10), allowing the free versus ATPγS-bound RecA filaments to be monitored indirectly.[79] We expected such protein-based fluorescence experiments to complement the DNA-based d6MI signals.

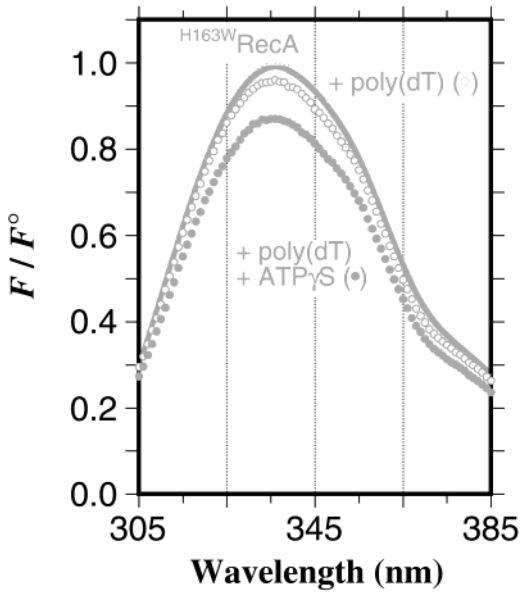

Figure 10. Influence of poly(dT) and ATPγS on the total fluorescence emission of ^{H163W}RecA protein. Normalized fluorescence emission spectra were collected for the protein alone (gray line) or in the presence of either poly(dT) (open symbols) or poly(dT) and ATPγS (filled symbols).

When the ^{H163W}RecA·ssDNA collapsed filament was rapidly mixed with ATPγS, real-time monitoring of intrinsic protein fluorescence revealed only a single slow phase (Figure 8, trace C).[80] The relaxation time for the observed quench of RecA emission was kinetically indistinguishable ($\tau = 7 \pm 2$ s) from the slower phase observed by DNA emission changes (14 ± 1 s). Rapid mixing of the binary ^{H163W}RecA·ATPγS complex with the ODN revealed only the slower, bimolecular association phase of the reaction (Figure 8, trace D; $\tau = 5 \pm 1$ s).

The results with ^{H163W}RecA allow the alternative hypotheses to be distinguished unambiguously. The fact that the protein-based signal change occurs on a time-scale slower than that of ssDNA dissociation uniquely supports the inference that ssDNA dissociation precedes the protein conformational change. Such a slow RecA conformational change has been observed during steady-state turnover of ATP.[77] We therefore propose the kinetic scheme for activation of the nucleoprotein filament shown in Figure 9 (lower pathway).[81]

The relative ordering of molecular events described in Figure 9—RecA·ssDNA dissociation followed by RecA conformational change—is further corroborated by the observation that mixing the collapsed nucleoprotein filament with a variety of nucleoside di- and triphosphates, including those that do not induce a protein conformational change (ADP[82] and dGTP[83]), induces only rapid ssDNA dissociation (data not shown). It is important to note that the DNA dissociation initiated by these nucleoside di- and triphosphates must be the result of binding and *not*

(70) Dombroski, D. F.; Scraba, D. G.; Bradley, R. D.; Morgan, A. R. *Nucl. Acids Res.* **1983**, *11*, 7487−7504.
(71) Eriksson, S.; Nordén, B.; Takahashi, M. *J. Biol. Chem.* **1993**, *268*, 1805−1810.
(72) Morrical, S. W.; Lee, J.; Cox, M. M. *Biochemistry* **1986**, *25*, 1482−1494.
(73) Stole, E.; Bryant, F. R. *J. Biol. Chem.* **1994**, *269*, 7919−7925.
(74) Maraboeuf, F.; Voloshin, O.; Camerini-Otero, R. D.; Takahashi, M. *J. Biol. Chem.* **1995**, *270*, 30927−30932.
(75) Morimatsu, K.; Horii, T.; Takahashi, M. *Eur. J. Biochem.* **1995**, *228*, 779−785.
(76) Morimatsu, K.; Funakoshi, T.; Horii, T.; Takahashi, M. *J. Mol. Biol.* **2001**, *306*, 189−199.
(77) Stole, E.; Bryant, F. R. *Biochemistry* **1997**, *36*, 3483−3490.
(78) Story, R. M.; Weber, I. T.; Steitz, T. A. *Nature* **1992**, *355*, 318−325.
(79) Rapid mixing of ^{H163W}RecA·ATPγS with ODN 30-6MI reveals DNA association kinetics identical to those of the wild-type protein.
(80) The observation of similar mechanistic behavior when the nucleoprotein filaments formed between ^{H163W}RecA and either ODN 30-G, $(dT)_{30}$, or poly-(dT) (221 nts in length) were mixed with ATPγS demonstrates that the observed changes are not an artifact associated with using an ODN or a specific sequence.
(81) Using the current data sets, we are unable to resolve the issue as to whether the protein conformational change is simultaneous with DNA association. Nevertheless, we have depicted the conformational change preceding association for illustrative purposes.
(82) Cox, M. M.; Soltis, D. A.; Lehman, I. R.; DeBrosse, C.; Benkovic, S. J. *J. Biol. Chem.* **1983**, *258*, 22586−22492.
(83) Menetski, J. P.; Varghese, A.; Kowalczykowski, S. C. *Biochemistry* **1988**, *27*, 1205−1212.

phosphate hydrolysis. Hence, we conclude that nucleotide *binding* is a general signal for ssDNA release by the collapsed RecA filament. The authentic signal is most likely generated by repulsive electrostatic or steric forces or both between the bound nucleotide and strand of DNA. These structural impedances to ssDNA binding must be relieved upon the conformational change to the extended RecA·ATPγS filament.

Functional Implications of Nucleotide-Induced DNA Dissociation. We have demonstrated that the RecA·ssDNA filament, unlike related hexameric motor protein assemblies, cannot be directly converted from the inactive to the active state by nucleotide binding-induced conformational change. Instead, a nucleotide binding results in the release of the bound DNA strand, then a conformational change of the DNA-free protomeric filament, and finally, reassociation of the activated protein filament with the DNA strand. This behavior contradicts expectations based on the structural similarity of RecA to hexameric motor proteins. We speculate that the functional significance of nucleotide-induced DNA dissociation from RecA filaments is related to the coincidence of switchlike activities (e.g., SOS induction following DNA damage) and motorlike activities (e.g., DNA strand exchange through heterologous sequences) in the same protein structure. In analogy to a recent[84] and controversial[85−87] proposal that bacterial mismatch repair proteins are ATP-dependent molecular switches, experiments are currently in progress to test hypotheses relating to the potential classification of RecA as an "A-protein".

In addition to providing a stark contrast with hexameric motor protein assemblies, these novel insights into the mechanism of RecA activation has several important implications. First, the requirement for an ATP-dependent protein conformational change prior to or concomitant with ssDNA binding provides a rationale for the observation that RecA·ssDNA association in the presence of ATPγS is much slower than in the absence of nucleotide cofactor. Second, the requirement for ATP-initiated ssDNA dissociation from the inactive filament provides a mechanistic basis for the observation that saturation of RecA with ATP does not produce a presteady-state burst of hydrolysis.[77] Finally, these conclusions provide a physical rationale for several qualitative observations in the RecA field, including (1) the ATP-induced changes in fluorescence from RecA-bound DNA containing ϵA,[56] (2) the ATP-dependent release of RecA from DNA−cellulose resin during purification,[88] and (3) the instability of RecA·DNA complexes upon cofactor addition in filter binding experiments.[89]

Conclusions

A major conclusion of this work is that the *dynamics* of RecA·ssDNA interactions are fundamentally different during the assembly of inactive ("collapsed") and active ("extended") RecA filaments. Although the collapsed filament formed in the absence of nucleotide cofactor assembles more than 50-fold faster than the active filament, the former complex, unlike related hexameric motor protein assemblies, cannot be directly converted from the inactive to the active state by a nucleotide binding-induced conformational change. Instead, nucleotide binding results in the release of the bound DNA strand, a conformational change of the DNA-free protomeric filament, and reassociation of the activated protein filament with the DNA strand. Our comparative studies of the collapsed and extended RecA filaments provide fundamental insights into the nature and dynamics of RecA·ssDNA interactions.

The characterization of nucleoprotein filament assembly based on the 6MI reporter demonstrates the significant advantages of this intrinsic DNA fluorophore over previous fluorescent reporters. Among the reasons why a complete mechanistic description of RecA-mediated DNA repair has remained elusive is the fact that no high-resolution structures of RecA·DNA complexes have been reported to date. In the absence of such structural data, sensitive and site-specific probes of real-time changes in RecA conformation and RecA·DNA interactions are needed.[29] One long-term objective of characterizing site-specific interactions among the filament constituents is to reach a molecular understanding of recombination and recombinational repair by the construction and elaboration of three-dimensional models of the intermediates in the reactions. Signal changes from site-specific structural and dynamic probes will be useful in conjunction with mechanistic models to elucidate structure−function relationships among RecA's diverse activities. The use of synthetic pteridine fluorophores in thermodynamic and kinetic studies promises to play a prominent role in a new era of biochemistry for RecA and related DNA molecular motors. Experiments are underway to construct a complete kinetic scheme describing RecA·ssDNA complex formation from which more challenging studies can emerge, such as elucidating the mechanism of homologous DNA recognition directed by RecA during recombinational repair.

Experimental Section

Materials. The *E. coli* RecA protein and the H163W mutant protein were overexpressed and purified from a nuclease deficient strain to >97% homogeneity as described[90] and stored in a 50% aqueous glycerol solution buffered by Tris at −80 °C. The wild-type RecA protein concentration was determined using the monomer extinction coefficient 2.2×10^4 $M^{-1}\cdot cm^{-1}$ at 280 nm.[91] The extinction coefficient for ^{H163W}RecA is 2.7×10^4 $M^{-1}\cdot cm^{-1}$ at 280 nm as determined by the method of Pace and co-workers.[92,93] The concentration of poly(dT) (Amersham-Pharmacia, average length 220 nts) was determined using the extinction coefficient 8520 $(M\text{-nts})^{-1}\cdot cm^{-1}$ at 264 nm.[94] The concentrations of ATP and ATPγS (both from Roche) were determined using the extinction coefficient 15 400 $M^{-1}\cdot cm^{-1}$ at 259 nm.[95] Lactic dehydrogenase, pyruvate kinase, NADH, and phosphoenolpyruvate were obtained from Sigma. Glycerol (spectrophotometric grade) was from Acros. Exonuclease I was from Epicentre Technologies.

(84) Fishel, R. *Genes Dev.* **1998**, *12*, 2096−2101.
(85) Blackwell, L. J.; Martik, D.; Bjornson, K. P.; Bjornson, E. S.; Modrich, P. *J. Biol. Chem.* **1998**, *273*, 32055−32062.
(86) Schofield, M. J.; Nayak, S.; Scott, T. H.; Du, C.; Hsieh, P. *J. Biol. Chem.* **2001**, *276*, 28291−28299.
(87) Blackwell, L. J.; Bjornson, K. P.; Allen, D. J.; Modrich, P. *J. Biol. Chem.* **2001**, *276*, 34339−34347.
(88) Cox, M. M.; McEntee, K.; Lehman, I. R. *J. Biol. Chem.* **1981**, *256*, 4676−4678.
(89) McEntee, K.; Weinstock, G. M.; Lehman, I. R. *J. Biol. Chem.* **1981**, *256*, 8835−8844.
(90) Berger, M. D.; Lee, A. M.; Simonette, R. A.; Jackson, B. E.; Roca, A. I.; Singleton, S. F. *Biochem. Biophys. Res. Commun.* **2001**, *286*, 1195−1203.
(91) Craig, N. L.; Roberts, J. W. *J. Biol. Chem.* **1981**, *256*, 8039−8044.
(92) Pace, C. N.; Vajdos, F.; Fee, L.; Grimsley, G.; Gray, T. *Protein Sci.* **1995**, *4*, 2411−2423.
(93) Pace; C. N.; Schmid, F. X. In *Protein Structure: A Practical Approach*, 2nd ed.; Creighton, T. E., Ed.; Oxford University Press: New York, 1997; p 253.
(94) Ts'o, P. O. P.; Rapaport, S. A.; Bollum, F. J. *Biochemistry* **1966**, *5*, 4153−4170.
(95) Bock, R. M.; Ling, N.-S.; Morell, S. A.; Lipton, S. H. *Arch. Biochem. Biophys.* **1956**, *62*, 253−264.

Oligodeoxyribonucleotide Preparation. The sequence of the 30mer ODNs [5′-TAGCTCCTTCGGTCCTCgATCGTTGTCAG, where g = d6MI (30-6MI) or g = G (30-G)] was derived from pGEM4Z (GenBank accession number X65305) coordinates 1685−1723.[96] ODN 30-6MI was synthesized and PAGE purified as described.[97] ODN 30-G was synthesized and PAGE purified by Integrated DNA Technologies. The concentrations of the ODNs were determined using extinction coefficients calculated by the nearest-neighbor method from the monomer and dimer values[98] and corrected for the extinction coefficient at 260 nm for d6MI (49 00 $M^{-1}\cdot cm^{-1}$).[97] The extinction coefficients at 260 nm for the nonfluorescent and d6MI-labeled 30mers were 2.47 and 2.41×10^5 $M^{-1}\cdot cm^{-1}$, respectively.

Steady-State Spectrofluorometry. Fluorescence data were collected on an SLM 8100 spectrofluorometer (SLM-Aminco) using (unless indicated otherwise) 3 μM-nts ODN, 4 μM RecA, and (when added) 100 μM ATPγS incubated for 10 min in aqueous buffer (25 mM Tris·HOAc, 4 mM $Mg(OAc)_2$, 5% w/v glycerol, 1 mM DTT, at a final pH of 7.1 ± 0.1 at 37.0 ± 0.1 °C). The total reaction volume of 650 μL was in a 2-mm × 10-mm cuvette oriented with the 2-mm path length parallel to the excitation beam to minimize inner filter effects. Further correction for the inner filter effect was not necessary since absorbance values at the excitation wavelength were below 0.05. For ODN 30-6MI, the excitation and emission wavelengths were 340 and 431 nm, respectively, with spectral bandwidths of 4 nm. The total emission intensities were corrected for dilution and protein effects, and were normalized by the fluorescence of the free ODN (F^o). The standard errors in the emission intensities were ±10%.

Protein fluorescence spectra were collected as described above except for the following changes. The substrates [10 μM-nts poly(dT), 1 μM ^{H163W}RecA, and (when added) 200 μM ATPγS] were incubated for 10 min in the aqueous buffer described above. The excitation wavelength was 295 nm with excitation and emission spectral bandwidths of 4 nm. The spectra were corrected for the buffer background and were normalized by the emission maximum of the free ^{H163W}RecA protein (F^o).

For the titration experiments, small aliquots of a concentrated stock of RecA protein were added to the cuvette containing the reactants described above. Then the sample was mixed by pipetting and equilibrated for at least 2 min with the shutters closed. The DNA binding isotherms were fit to the full equation derived from the mass balance equations for bimolecular association between RecA(·ATPγS) and ssDNA:

$$Y = Y^o + \left(n\frac{\Delta Y}{2D_0}\right)\left\{\left(R_0 + \frac{D_0}{n} + K_d\right) - \left[\left(R_0 + \frac{D_0}{n} + K_d\right)^2 - 4R_0\frac{D_0}{n}\right]^{1/2}\right\}$$

where Y is the observed fluorescence value (F/F^o), Y^o is the initial fluorescence value (1 for the F data), ΔY is the total change in the fluorescence property, R_0 is the initial concentration of RecA protein, D_0 is the initial concentration of ssDNA in nucleotides, n is the number of nucleotides bound per RecA monomer, and K_d is the average apparent dissociation constant for the complex between a RecA(·ATPγS) monomer and n nucleotides of ssDNA. A dissection of the relative contributions of intrinsic affinity and cooperativity[48,99] are beyond the scope of this analysis.

For anisotropy data collection (r), the excitation beam was polarized with a Glan−Thompson polarizing prism oriented in the vertical direction. The excitation wavelength was 357 nm with a band-pass of 8 nm. A T-format fluorometer arrangement allowed the simultaneous collection of vertically and horizontally polarized emission using appropriately oriented prisms. The fluorescence emission was collected through long-pass filters with a cutoff at 420 nm (Oriel 59480). The intensity signals were corrected for dilution effects and background protein fluorescence before the anisotropy value was calculated in the usual manner: $r = (I_{||} - I_\perp)/(I_{||} + 2\cdot I_\perp)$. The standard errors for the r-values are ±0.006.

Stopped-Flow Spectrofluorometry. An SX.18MV stopped-flow spectrofluorometer (dead time ≤ 1.8 ms, Applied Photophysics Ltd, Leatherhead, UK) in "oversampling" mode was used to monitor the time-dependent fluorescence emission upon mixing RecA protein with ODN. The concentrations reported are the final concentrations in the flow cell after mixing. Both reactants were incubated in either the absence or presence of 500 μM ATPγS prior to mixing. All reactions were performed under the same solution conditions as the steady-state experiments described above with degassed and filtered water. Frozen reactants were thawed on ice and then incubated for at least 5 min in the stopped-flow at 37.0 ± 0.1 °C before mixing. Total fluorescence emission was collected through a long-pass filter with a cutoff at 420 nm (Oriel 51280) while the excitation wavelength was 356 nm (4-nm slit). The total emission intensities were normalized by the maximum observed fluorescence (F_{max}). Kinetic traces used in the figures or for subsequent data analysis were the average of at least three independent runs. Nonlinear least-squares fitting analysis of the kinetic traces was accomplished with the software provided by Applied Photophysics and KaleidaGraph (Synergy Software). Trial fittings with single-exponential and higher-order exponential functions were attempted. The time-dependent data were well described by single-exponential functions. Although more exponential terms gave rise to slightly better descriptions (judged by reduced χ^2 analysis), the improvements were modest and were accompanied by a reduction in the confidence intervals of the fitting parameters. Hence, we chose single-exponential functions in accord with the models derived from Schemes 1 and 2.

Stopped-flow experiments with the ^{H163W}RecA protein were collected and analyzed as above with the following modifications. Total fluorescence emission was collected through a long-pass filter with a cutoff at 370 nm (Corion LG-370) while the excitation wavelength was 295 nm (4-nm slit). The total emission intensities were normalized by the maximum observed fluorescence (F_{max}).

Acknowledgment. This work was supported by grants to S.F.S. from the NIH (GM58114) and the Welch Foundation (C-1374), and an NSF Minority Postdoctoral Research Fellowship to A.I.R. We are grateful to Mary E. Hawkins (NIH) for helpful discussions and for the initial preparation of ODN 30-6MI.

JA0270165

(96) Podyminogin, M. A.; Meyer, R. B.; Gamper, H. B. *Biochemistry* **1995**, *34*, 13098−13108.
(97) Hawkins, M. E.; Pfleiderer, W.; Mazumder, A.; Pommier, Y. G.; Balis, F. M. *Nucl. Acids Res.* **1995**, *23*, 2872−2880.
(98) Borer, P. N. In *Handbook of Biochemistry and Molecular Biology: Nucleic Acids*; Fasman, G. D., Ed.; CRC Press: Cleveland, OH, 1975; Vol. I, p 589.
(99) Takahashi, M.; Strazielle, C.; Pouyet, J.; Daune, M. *J. Mol. Biol.* **1986**, *189*, 711−714.